Dalton Transactions

PAPER

View Article Online
View Journal | View Issue

Cite this: *Dalton Trans.*, 2016, **45**, 17206

Synthesis, characterization, and ligand behaviour of a new ditelluroether $(C_{10}H_7)Te(CH_2)_4Te(C_{10}H_7)$ and the concurrently formed ionic $[(C_{10}H_7)Te(CH_2)_4]Br$†

Merja J. Poropudas, J. Mikko Rautiainen, Raija Oilunkaniemi and Risto S. Laitinen*

The reaction of 1-naphthyl bromide with *n*-butyl lithium, elemental tellurium, and 1,4-dibromobutane in THF affords both $(C_{10}H_7)Te(CH_2)_4Te(C_{10}H_7)$ (**1**) and $[(C_{10}H_7)Te(CH_2)_4]Br$ (**2**) in good yields. **1** is preferentially formed at low temperatures and is a rare example of a structurally characterized ditelluroether in which the tellurium atoms are bridged by a hydrocarbon chain. In the solid state, **1** shows secondary bonding Te···Te interactions, which connect the molecules into layers which are further linked to 3-dimensional frameworks by Te···H hydrogen bonds. $[(C_{10}H_7)Te(CH_2)_4]Br$ (**2**) is formed concurrently during the synthesis of **1** and is the main product, when the reaction is carried out at room temperature. The revPBE/def2-TZVPP calculations of the reaction profiles indicate that the formation of **2** is somewhat more favourable than that of **1**. Furthermore, at room temperature the activation energy for the formation of **2** is lower than that of **1**. At low temperatures the activation energy of the reaction leading to **1** is lower than that to **2**, which is consistent with the synthetic observations. When **1** was treated with CuBr, $[Cu_2(\mu\text{-}Br)_2\{\mu\text{-}(C_{10}H_7)Te(CH_2)_4Te(C_{10}H_7)\}_2]$ (**3**) was formed. It crystallizes as two polymorphs (**3a**) and (**3b**) in which both the packing and the conformation of the ditelluroether ligands are different. The reaction of **1** with $HgCl_2$ produces $[(C_{10}H_7)Te(CH_2)_4]_2[HgCl_4]\cdot CH_2Cl_2$ (**4**·CH_2Cl_2) and that of **1** with $CuCl_2$ affords $[(C_{10}H_7)Te(CH_2)_4]Cl$ (**5**). **2** and **5** are isomorphous.

Received 29th June 2016,
Accepted 19th September 2016

DOI: 10.1039/c6dt02599d

www.rsc.org/dalton

Introduction

Although the first preparation of ditelluroethers $RTe(CH_2)TeR$ (R = 4-MeO-C_6H_4, 4-EtO-C_6H_4, C_6H_5, $C_6H_5CH_2$, 4-Me-C_6H_4) from diazomethane and ditellurides dates back to the 1970s,[1] the chemistry of polytelluroethers has seen much slower progress than that of the related polythio- and polyselenoethers (for reviews, see ref. 2). Levason and Reid[2f] inferred that the difficulty in the preparation of di- and polytelluroether ligands is due to the inherent instability of Te–H bonds, which hinders the use of tellurols (RTeH) as synthons, the weakness of the Te–C bond leading to its facile cleavage, and the stability of the +IV oxidation state of tellurium.

In addition to the reaction between diazomethane and ditellurides,[1,3] $RTe(CH_2)_nTeR$ (R = Ph,[4] *p*-$EtOC_6H_4$,[4a] or Me;[4b,c] n = 1, 3) have been prepared by the reaction of RTe^- with organic dihalides $X(CH_2)_nX$ (X = Cl, Br) at low temperatures. The reaction, however, is dependent on the starting materials and reaction conditions. At room temperature, the reaction of RTe^- and $X(CH_2)_nX$ (n = 2 or 3) afforded R_2Te_2 and alkenes.[4] Interestingly, it has also been reported that the reaction of (4-$EtOC_6H_4$)TeNa and $X(CH_2)_nX$ (X = Br or I; n = 3 or 4) in aqueous ethanol does not yield the ditelluroether (4-$EtOC_6H_4$)-$Te(CH_2)_nTe$(4-$EtOC_6H_4$), because of the faster formation of the telluronium salt $[(4\text{-}EtOC_6H_4)Te(CH_2)_n]X$.[4a] It is only with the chain lengths of n = 6–10 that the related reaction affords (4-$EtOC_6H_4$)$Te(CH_2)_nTe$(4-$EtOC_6H_4$).[5] In the case of $X(CH_2)_5X$, both the ditelluroether and the telluronium halogenide are obtained. Furthermore, the treatment of RTe^- with $X(CH_2)_4X$ (R = Me, Ph; X = Cl, Br) resulted in a mixture of R_2Te and cyclic tetrahydrotellurophene, $Te(CH_2)_4$, while that of $Cl(CH_2)_5Cl$ afforded a mixture of $RTe(CH_2)_5TeR$, R_2Te, and $Te(CH_2)_4$.[4c]

All the above-mentioned products have been identified and characterized by NMR and mass spectroscopy[3a,4,5] and in some cases by ^{125}Te Mössbauer spectroscopy.[3a,4a] The only known crystal structures of ditelluroethers $RTe(CH_2)_nTeR$ are those of $[4\text{-}MeO(C_6H_4)Te)]_2CH_2$ [6a,b] and bis(2-fluoro-3-pyridyltelluro)methane.[6c] The crystal structures of some transition

Laboratory of Inorganic Chemistry, University of Oulu, P. O. Box 3000, FI-90014 Oulu, Finland. E-mail: risto.laitinen@oulu.fi

†Electronic supplementary information (ESI) available: Shortest interionic contacts and packing of **2**, **3a**, **3b**, **4**, and **5**, the XYZ files of PBE0/def2-TZVPP optimized structures, and the CIF-file of the PBE0/pop-TZVP optimized crystal structure of **2**. CCDC 1487835–1487840. For ESI and crystallographic data in CIF or other electronic format see DOI: 10.1039/c6dt02599d

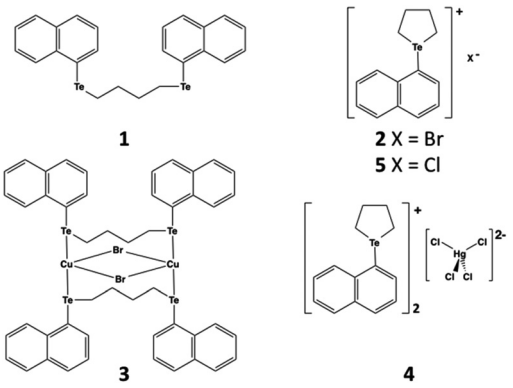

Chart 1 $(C_{10}H_7)Te(CH_2)_4Te(C_{10}H_7)$ (**1**), $[(C_{10}H_7)Te(CH_2)_4]X$ [X = Br(**2**), Cl (**5**)], $[Cu_2(\mu\text{-}Br)_2\{\mu\text{-}(C_{10}H_7)Te(CH_2)_4Te(C_{10}H_7)\}_2]$ (**3**), and $[C_{10}H_7Te(CH_2)_4]_2[HgCl_4]$ (**4**).

metal complexes with chelating[6b,7] or bridging[6b,8] RTe$(CH_2)_n$TeR (n = 1 or 3) ligands have also been determined. Monotelluroethers R_2Te (R = C_6H_5, C_4H_3S, Me_3SiCH_2) have also been shown to form versatile metal complexes with silver(I) and copper(I).[9]

In this contribution, we report the low-temperature synthesis and structural characterization of naphthyl ditelluroether $(C_{10}H_7)Te(CH_2)_4Te(C_{10}H_7)$ (**1**). Upon prolonged reaction time and at a higher temperature, $[(C_{10}H_7)Te(CH_2)_4]Br$ (**2**) is obtained as a main product. The factors affecting the concurrent formation of **1** and **2** have been discussed on the basis of DFT calculations. We have also explored the ligand behavior of **1**. When $(C_{10}H_7)Te(CH_2)_4Te(C_{10}H_7)$ (**1**) reacts with CuBr, an unprecedented dinuclear Cu(I) complex $[Cu_2(\mu\text{-}Br)_2\{\mu\text{-}(C_{10}H_7)Te(CH_2)_4Te(C_{10}H_7)\}_2]$ (**3**) is formed. The reaction of **1** with $HgCl_2$ produces $[(C_{10}H_7)Te(CH_2)_4]_2[HgCl_4]$ (**4**) containing a similar Te-cation to that in **2**. All compounds have been characterized by single-crystal X-ray diffraction and NMR spectroscopy. The structural formulae of **1–4** have been depicted in Chart 1.

Experimental

General

All reactions and manipulations of air- and moisture-sensitive reagents were carried out under an argon atmosphere. Tellurium (Aldrich), *n*-BuLi (Aldrich), $HgCl_2$ (Merck), and $CuCl_2$ (Aldrich) were used as purchased. 1,4-Dibromobutane (Aldrich) and 1-bromonaphthalene (Merck) were dried with molecular sieves and bubbled with argon prior to use. CuBr was prepared according to a literature method.[10] All solvents were dried and distilled under an argon atmosphere prior to use. Tetrahydrofuran (Lab-Scan) and diethyl ether (Lab-Scan) were dried over Na/benzophenone and dichloromethane (Lab-Scan) over P_4O_{10}.

NMR spectroscopy

$^{13}C\{^1H\}$ and ^{125}Te NMR spectra were recorded unlocked in CH_2Cl_2 on a Bruker Avance III spectrometer operating at 100.62 MHz and 126.29 MHz, respectively. The typical respective spectral widths were 24.04 kHz and 125.00 kHz. The pulse widths were 4.8 μs and 8.17 μs, respectively. The $^{13}C\{^1H\}$ pulse delay was 6.50 s and that for ^{125}Te was 1.60 s. $^{13}C\{^1H\}$ accumulations contained *ca.* 1000 transients and those for ^{125}Te 30 000 transients. The ^{13}C spectra were referenced to the solvent resonance and are reported relative to Me_4Si. For ^{125}Te, a saturated solution of H_6TeO_6 (aq.) was used as an external reference. The ^{125}Te chemical shifts are reported relative to neat Me_2Te [$\delta(Me_2Te) = \delta(H_6TeO_6) + 712$].[11]

X-ray crystallography

Diffraction data of **1–5** were collected on a Bruker Nonius Kappa-CCD diffractometer using graphite monochromated Mo K_α radiation (λ = 0.71073 Å; 55 kV, 25 mA). Crystal data and the details of the structure determinations are given in Table 1.

Structures were solved by direct methods using SHELXS-2013 and refined using SHELXL-2013.[12] After the full-matrix least-squares refinement of the non-hydrogen atoms with anisotropic thermal parameters, the hydrogen atoms were placed in calculated positions in the aromatic rings (C–H = 0.95 Å), and in the CH_2 groups (C–H = 0.99 Å). The scattering factors for the neutral atoms were those incorporated with the programs.

One naphthyl group in **1** is disordered with two alternative orientations. This disorder was resolved in terms of two alternative orientations for the fused aromatic ring. The site occupation factors were refined by constraining the anisotropic displacement parameters of the disordered pairs of atoms to be equal.

Syntheses

$(C_{10}H_7)Te(CH_2)_4Te(C_{10}H_7)$ (1). Lithium naphthalenide was prepared according to a slightly modified literature procedure.[13] 1-Bromonaphthalene (1.75 mL, 12.5 mmol) was dissolved in 50 mL of diethylether. The solution was cooled to −40 °C and *n*-BuLi (5.00 mL of 2.5 M in hexanes, 12.5 mmol) was added. The solution was stirred for 1.5 hours at −40 °C during which a white precipitate of lithium naphthalenide was formed. The ether solution was decanted after which the precipitate was washed with 100 mL of dry hexane and dried under vacuum.

Lithium naphthalenide was dissolved in 50 mL of THF and the solution was cooled to −50 °C. Freshly ground tellurium (1.616 g, 12.67 mmol) was added. The solution was stirred for 1.5 hours during which the temperature of the solution rose to −25 °C, and 1,4-dibromobutane (0.75 mL, 6.28 mmol) was added. The orange red solution quickly turned yellow. After one hour the reaction solution was filtered and the solvent was evaporated. The residue was dissolved in dichloromethane and filtered. The filtrate was concentrated and cooled during which a light yellow precipitate of $(C_{10}H_7)Te(CH_2)_4Te(C_{10}H_7)$ (**1**) was formed. Crystallization from THF afforded light yellow crystals of **1** suitable for X-ray crystallography. Yield: 1.747 g (49%, based on *n*-BuLi). Anal. calc. for $C_{24}H_{22}Te_2$: C 50.96, H 3.92; found: C 50.42, H 3.78%. ^{125}Te-NMR(CH_2Cl_2): 352 ppm.

Table 1 Crystal data and details of the structure determinations of $(C_{10}H_7)Te(CH_2)_4Te(C_{10}H_7)$ (**1**), $[(C_{10}H_7)Te(CH_2)_4]Br$ (**2**), $[Cu_2(\mu\text{-}Br)_2\{\mu\text{-}(C_{10}H_7)Te(CH_2)_4Te(C_{10}H_7)\}_2]$ (**3a**, **3b**), $[(C_{10}H_7)Te(CH_2)_4]_2[HgCl_4]\cdot CH_2Cl_2$ (**4**), and $[(C_{10}H_7)Te(CH_2)_4]Cl$ (**5**)

	1	2	3a	3b	4	5
Empirical formula	$C_{24}H_{22}Te_2$	$C_{14}H_{15}BrTe$	$C_{48}H_{44}Br_2Cu_2Te_4$	$C_{48}H_{44}Br_2Cu_2Te_4$	$C_{29}H_{32}Cl_6HgTe_2$	$C_{14}H_{15}ClTe$
Relative molecular mass	565.61	390.77	1418.13	1418.13	1049.04	346.31
Crystal system	Monoclinic	Orthorhombic	Triclinic	Monoclinic	Triclinic	Orthorhombic
Space group	$C2/c$	$P2_12_12_1$	$P\bar{1}$	$P2_1/c$	$P\bar{1}$	$P2_12_12_1$
a (Å)	17.921(4)	7.2568(15)	7.425(5)	15.679(3)	10.815(2)	7.1073(14)
b (Å)	17.872(4)	12.253(3)	11.072(5)	12.479(3)	12.255(3)	11.861(2)
c (Å)	26.204(5)	15.227(3)	14.288(5)	11.389(2)	13.905(3)	15.403(3)
α (°)			91.048(5)		64.29(3)	
β (°)	93.38(3)		101.586(5)	96.32(3)	81.58(3)	
γ (°)			106.987(5)		89.23(3)	
V (Å^3)	8378(3)	1353.9(5)	1096.8(10)	2214.9(8)	1639.9(7)	1298.4(5)
T (K)	150(2)	150(2)	150(2)	120(2)	150(2)	150(2)
Z	16	4	1	2	2	4
F(000)	4320	744	668	1336	984	672
$D_{calc.}$ (g cm^{-3})	1.794	1.917	2.147	2.126	2.124	1.772
μ(Mo-K$_\alpha$) (mm^{-1})	2.790	5.120	5.432	5.380	6.944	2.467
Crystal size (mm)	0.20 × 0.10 × 0.04	0.30 × 0.05 × 0.03	0.15 × 0.10 × 0.01	0.15 × 0.15 × 0.01	0.20 × 0.15 × 0.02	0.20 × 0.10 × 0.02
θ range (°)	3.12–25.00	3.11–25.98	2.94–25.00	2.85–25.00	2.96–26.00	3.15–25.99
No. of reflns collected	21 188	8119	12 420	23 226	20 995	7365
No. of unique reflns.	7346	2598	3619	3706	6186	2528
No. of observed reflns[a]	5026	2092	3062	3225	5382	2345
No. of parameters/ restraints	443/24	145/0	257/0	253/0	344/0	147/0
R_{INT}	0.0923	0.0670	0.0641	0.0864	0.0679	0.0696
R_1[a]	0.0927	0.0457	0.0382	0.0606	0.0447	0.0469
wR_2[b]	0.1600	0.0687	0.0797	0.1215	0.1013	0.0979
R_1 (all data)[a]	0.1432	0.0713	0.0529	0.0737	0.0555	0.0550
wR_2 (all data)[b]	0.1789	0.0763	0.0852	0.1283	0.1074	0.1040
GOF on F^2	1.170	1.101	1.103	1.026	1.105	1.160
$\Delta\rho_{max,min}$ (e Å^{-3})	3.909, −2.057	0.551, −0.560	0.962, −0.737	4.395, −1.383	2.401, −1.715	0.911, −0.656

[a] $I \geq 2\sigma(I)$. [b] $R_1 = \sum||F_o| - |F_c||/\sum|F_o|$, $wR_2 = [\sum w(F_o^2 - F_c^2)^2/\sum wF_o^4]^{1/2}$.

^{13}C-NMR(CH_2Cl_2): 138.1, 136.0, 133.2, 131.7, 128.6, 128.4, 126.4, 125.9, 125.8, 115.0, 33.4, 7.1 ppm.

$[(C_{10}H_7)Te(CH_2)_4]Br$ (2). $[(C_{10}H_7)Te(CH_2)_4]Br$ (**2**) was prepared as previously described for $(C_{10}H_7)Te(CH_2)_4Te(C_{10}H_7)$ (**1**) using 1-bromonaphthalene (1.75 mL, 12.5 mmol), *n*-BuLi (5.00 mL, 12.5 mmol), tellurium (1.621 g, 12.70 mmol), and 1,4-dibromobutane (0.75 mL, 6.28 mmol). In this case, the reaction mixture was stirred overnight instead of one hour. During this time the solution was allowed to warm slowly to room temperature.

The solvent in the yellow brownish reaction mixture was evaporated. The residue was dissolved in dichloromethane (60 mL), filtered, and the solvent was evaporated. A white precipitate was formed upon dissolving the residue in THF. After filtration and washing the precipitate with THF and hexane, followed by recrystallization from CH_2Cl_2, colourless crystals of $[(C_{10}H_7)Te(CH_2)_4]Br$ (**2**), which were suitable for X-ray structure determination, were obtained. Yield: 0.973 g (40%, based on lithium naphthalenide). Anal. calc. for $C_{14}H_{15}BrTe$: C 43.03, H 3.87; found: C 42.79, H 3.72%. ^{125}Te-NMR(CH_2Cl_2): 666 ppm. ^{13}C-NMR(CH_2Cl_2): 134.0, 133.5, 131.8, 131.0, 129.2, 127.4, 126.5, 126.2, 125.9, 123.3, 39.6, 32.5 ppm.

The THF filtrate was evaporated and dissolved in dry CH_2Cl_2. Upon concentration and cooling of the solution, a light yellow precipitate of $(C_{10}H_7)Te(CH_2)_4Te(C_{10}H_7)$ (**1**) was formed. Yield: 0.804 g (23% based on lithium naphthalenide).

$[Cu_2(\mu\text{-}Br)_2\{\mu\text{-}(C_{10}H_7)Te(CH_2)_4Te(C_{10}H_7)\}_2]$ (3). $(C_{10}H_7)Te(CH_2)_4Te(C_{10}H_7)$ (**1**) (0.294 g, 0.520 mmol) was dissolved in dichloromethane (5 mL) and added into a flask containing CuBr (0.060 g, 0.418 mmol) and 2 mL of dichloromethane. The solution was stirred for 3 hours. A light yellow precipitate was isolated and washed with dichloromethane. Colourless crystals of $[Cu_2(\mu\text{-}Br)_2\{\mu\text{-}(C_{10}H_7)Te(CH_2)_4Te(C_{10}H_7)\}_2]$ (**3a** and **3b**) suitable for single crystal X-ray diffraction were formed in a dilute CH_2Cl_2 solution. Yield: 0.297 g (94%, based on CuBr). Anal. calc. for $C_{24}H_{22}BrCuTe_2$: C 40.65, H 3.13; found: C 40.22, H 3.14%. ^{125}Te-NMR(CH_2Cl_2): 660 ppm.

$[(C_{10}H_7)Te(CH_2)_4]_2[HgCl_4]\cdot CH_2Cl_2$ (4·CH_2Cl_2). $(C_{10}H_7)Te(CH_2)_4Te(C_{10}H_7)$ (**1**) (0.160 g, 0.283 mmol) was dissolved in dichloromethane (5 mL) and added into a flask containing $HgCl_2$ (0.077 g, 0.284 mmol) and 2 mL of dichloromethane. The reaction mixture was stirred overnight. The cloudy bright yellow solution was filtered. Upon concentration and cooling, a light yellow precipitate was formed. The precipitate was washed with cold dichloromethane. X-ray-quality crystals of $[(C_{10}H_7)Te(CH_2)_4]_2[HgCl_4]\cdot CH_2Cl_2$ (**4**·CH_2Cl_2) were obtained by recrystallization from CH_2Cl_2 at 0 °C. Yield: 0.081 g

(54%, based on 1). Anal. calc. for $C_{29}H_{32}Cl_6HgTe_2$: C 33.20, H 3.07; found: C 33.48, H 2.98%. ^{125}Te-NMR(CH_2Cl_2): 680 ppm.

[$(C_{10}H_7)$Te$(CH_2)_4$]Cl (5). $(C_{10}H_7)Te(CH_2)_4Te(C_{10}H_7)$ (**1**) (0.220 g, 0.389 mmol) was added into a flask containing $CuCl_2$ (0.035 g, 0.260 mmol) and 8 mL of dichloromethane. The reaction mixture was stirred for three hours and the cloudy bright yellow solution was filtered. The white precipitate was washed with cold dichloromethane. X-ray-quality crystals of [$(C_{10}H_7)$Te$(CH_2)_4$]Cl (**5**) were obtained by recrystallization from acetonitrile at 0 °C.

Computational details

All structures considered in this work were optimized with the ORCA program using gradient techniques[14] and employing a revPBE GGA functional[15] and def2-TZVPP[16] basis sets together with the RI approximation[17] and Grimme's dispersion corrections.[18] Energies for species in THF were calculated using the COSMO polarizable continuum model[19] implemented in ORCA. The fundamental frequencies were calculated to assess the nature of stationary points and to estimate the zero-point energy (ZPE) corrections and Gibbs reaction energies. The reported transition states correspond to structures with a single imaginary vibrational mode along the reaction coordinate.

To account for the formation of solid [$(C_{10}H_7)$Te$(CH_2)_4$]Br in the reaction, the formation of the ion pair [$(C_{10}H_7)$Te$(CH_2)_4$]$^+$ and Br^- was computed at the revPBE/def2-TZVPP level and corrected for lattice effects by estimating the sublimation energy using solid-state DFT calculations. The Crystal14 program package,[20] which utilizes periodic boundary conditions, and the PBE0 functional[15a,b,21] were employed for solid-state DFT calculations. Triple-zeta valence basis sets that are designed for solid-state calculations and include polarization functions pob-TZVP[22] were used for all other elements except for tellurium, for which a locally modified basis set was used.[23] Grimme's corrections as implemented in Crystal14 were employed to account for dispersion interactions.[24] The Hamiltonian matrix was diagonalized in a set of *k*-points in a reciprocal space generated according to the Pack–Monkhorst method for sampling the first Brillouin zone with a shrinking factor (4, 4). For the evaluation of Coulomb and exchange integrals (TOLINTEG), tolerance factors of 8, 8, 8, 8, and 16 were used.[25] The default SCF convergence threshold on total energy (10^{-7} hartree) was used for optimizations while for frequency calculations the threshold was increased to 10^{-11} hartree. Vibrational corrections to energies for the crystal structure were determined using harmonic phonon frequencies calculated at the Γ-point of the Brillouin zone without considering phonon dispersion.[25]

Results and discussion

General

At low temperatures, $(C_{10}H_7)Te(CH_2)_4Te(C_{10}H_7)$ (**1**) was obtained in moderate yields from 1-bromonaphthalene, as shown in Scheme 1. After the addition of 1,4-dibromobutane, the workup and isolation of **1** was carried out in 1 h. Pure **1** is relatively stable under argon. In solution, the compound shows two-fold symmetry. Consequently, the NMR spectra in CH_2Cl_2 exhibit one ^{125}Te resonance at 352 ppm and twelve ^{13}C resonances. Ten resonances at 138.1–115.0 ppm are attributable to the carbon atoms in the naphthyl group and those at 33.4 and 7.1 ppm are due to the two inequivalent CH_2 groups in the $(CH_2)_4$ chain.

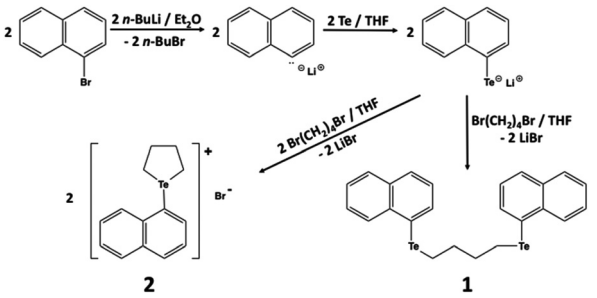

Scheme 1 Formation of $(C_{10}H_7)Te(CH_2)_4Te(C_{10}H_7)$ (**1**) and [$(C_{10}H_7)$Te$(CH_2)_4$]Br (**2**).

Upon prolonged stirring of the reaction mixture during which time the temperature was allowed to rise to ambient temperature, a white precipitate of [$(C_{10}H_7)$Te$(CH_2)_4$]Br (**2**) was observed. It is stable in air. The precipitate can be dissolved in CH_2Cl_2 and the NMR spectra show a ^{125}Te resonance at 666 ppm, ten ^{13}C resonances at 134.0–123.3, and two resonances at 39.6 and 32.5 ppm.

Our findings support the inferences of De Silva *et al.*[4a] that the room temperature synthesis of $RTe(CH_2)_nTeR$ (R = *p*-$EtOC_6H_4$, Ph; *n* = 3, 4) failed because of the formation of telluronium salts due to the internal quaternarization, which was always faster than the nucleophilic attack by RTe^- on the second C–Br bond of the precursor $Br(CH_2)_nBr$. We also concur that at room temperature the formation of the telluronium bromide **2** is faster than that of the ditelluroether **1** (see Scheme 1). The latter, however, seems to form more rapidly at low temperatures. In principle it is also possible that at higher temperatures the decomposition of **1** also takes place as shown in Scheme 2 producing additional telluronium bromide **2**.

The reaction of **1** with CuBr in a molar ratio 1 : 1 produced a dinuclear complex $[Cu_2(\mu\text{-}Br)_2\{\mu\text{-}(C_{10}H_7)Te(CH_2)_4Te(C_{10}H_7)\}_2]$ (**3**) in which two ditelluroether ligands and bromide ligands bridge two copper(I) centers (see Chart 1). **3** crystallized as two polymorphs **3a** and **3b**. There are a few bidental phosphane complexes, which contain similar structures where both the phosphane and halogenido ligands bridge two Cu(I) centers.[26]

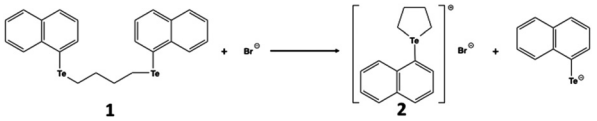

Scheme 2 Possible decomposition of $(C_{10}H_7)Te(CH_2)_4Te(C_{10}H_7)$ (**1**).

The reaction of **1** with $CuCl_2$ afforded colourless crystals of $[(C_{10}H_7)Te(CH_2)_4]Cl$ (**5**) and red crystals of $(C_{10}H_7)_2Te_2$. The crystal structure of the latter is known.[27]

The reaction of $(C_{10}H_7)Te(CH_2)_4Te(C_{10}H_7)$ (**1**) and $HgCl_2$ in CH_2Cl_2 afforded $[(C_{10}H_7)Te(CH_2)_4]_2[HgCl_4]\cdot CH_2Cl_2$ (**4**·CH_2Cl_2), which also contains the $[(C_{10}H_7)Te(CH_2)_4]^+$ cation like **2** and **5**. The preparation of $(Ph_3Te)_2[HgCl_4]$,[28] $(Ph_3Te)_2[Hg_2Cl_6]$,[29a] and $(RTe)_2[Hg_2Cl_6]$ {R = 2,6-$[O(CH_2CH_2)_2NCH_2]_2C_6H_3$}[29b] has also been reported, though only the $[Hg_2Cl_6]^{2-}$ salts have been structurally characterized.

Crystal structures

$(C_{10}H_7)Te(CH_2)_4Te(C_{10}H_7)$ (1) and $[C_{10}H_7Te(CH_2)_4]_nX$ {*n* = 1, X = Br (2), Cl (5); *n* = 2, X = $[HgCl_4]$ (4)}. The molecular structure of $(C_{10}H_7)Te(CH_2)_4Te(C_{10}H_7)$ (**1**) indicating the numbering of atoms and selected bond parameters is shown in Fig. 1.

The asymmetric unit in **1** contains two molecules. Te–C bond distances span a range of 2.118(9) Å–2.186(16) Å, which are comparable to those reported for bis(4-methoxyphenyltelluro)methane [2.13(2) Å–2.15(2) Å].[6b] The C–Te–C bond angles are 89.5(8)–95.0(3)°. The naphthyl group, which is bonded to Te4, is disordered with the ring assuming two different orientations [s.o.f. 0.547(11) and 0.453(11); see Fig. 1].

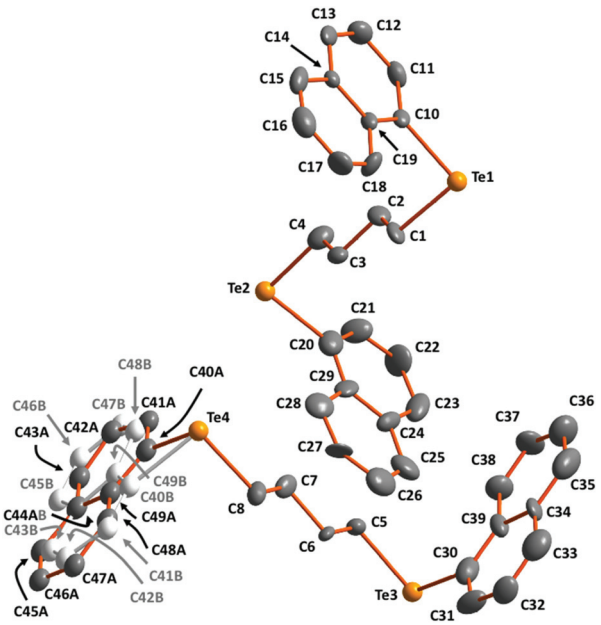

Fig. 1 The molecular structure of $(C_{10}H_7)Te(CH_2)_4Te(C_{10}H_7)$ (**1**) indicating the numbering of atoms. Thermal ellipsoids have been drawn at 50% probability level. The atoms in the more abundant of the disordered pair of the naphthyl group [C40A–C49A; s.o.f. 0.547(11)] in **1** are shown in color, whereas those in the less abundant group [C40B–C49B; s.o.f. 0.453(11)] are shown in white. Hydrogen atoms have been omitted for clarity. Selected bond lengths (Å) and angles (°): Te1–C1 2.161(11), Te1–C10 2.141(12), Te2–C4 2.153(15), Te2–C20 2.186(16), Te3–C5 2.164(12), Te3–C30 2.150(14), Te4–C8 2.156(13), Te4–C40A 2.118(9), Te4–C40B 2.130(9), C1–Te1–C10 94.4(5), C4–Te2–C20 92.2(6), C5–Te3–C30 95.0(3), C8–Te4–C40A 94.8(7), C8–Te4–C40B 89.5(8).

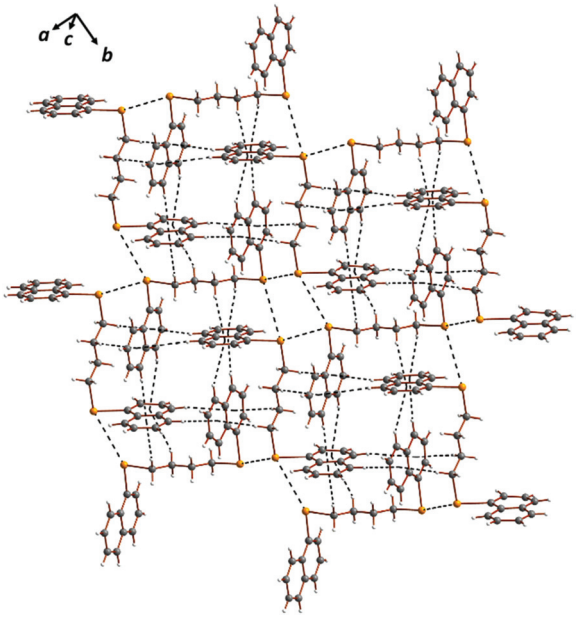

Fig. 2 The Te···Te and H···Np (Np = naphthyl) π close contacts connecting the individual $(C_{10}H_7)Te(CH_2)_4Te(C_{10}H_7)$ (**1**) molecules into a three-dimensional supramolecular network.

Each tellurium atom is involved in two intermolecular Te···Te interactions and a number of H···Np (Np = naphthyl) π close contacts. These interactions link the discrete molecules into a three-dimensional supramolecular network (see Fig. 2). The Te···Te contacts span a range of 3.9124(15)–4.0718(16) Å (the sum of van der Waals radii of two tellurium atoms is 4.40 Å (ref. 30)) and those for the H···Np hydrogen bonds involving the π electrons of the naphthyl rings show a range of 2.5350(4)–3.5111(6) Å.

Compounds $[(C_{10}H_7)Te(CH_2)_4]X$ [X = Br (**2**), Cl (**5**)] are isomorphous. The molecular structure indicating the labeling of atoms is shown in Fig. 3. The crystal structure of $[(C_{10}H_7)Te(CH_2)_4]_2[HgCl_4]\cdot CH_2Cl_2$ (**4**·CH_2Cl_2) is shown in Fig. 4.

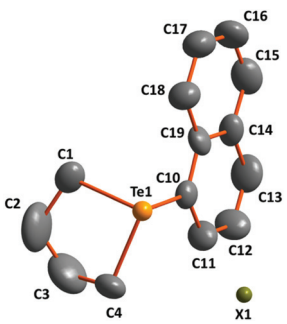

Fig. 3 The molecular structure of $[(C_{10}H_7)Te(CH_2)_4]X$ [X = Br (**2**), Cl (**5**)] indicating the numbering of atoms. Thermal ellipsoids have been drawn at 50% probability level. Hydrogen atoms have been omitted for clarity. Selected bond lengths (Å) and angles (°): **2**: Te1–C1 2.130(11), Te1–C4 2.122(10), Te1–C10 2.161(10), C1–Te1–C4 85.4(4), C1–Te1–C10 92.2(4), C4–Te1–C10 96.1(4); **5**: Te1–C1 2.109(12), Te1–C4 2.168(13), Te1–C10 2.147(12), C1–Te1–C4 84.1(5), C1–Te1–C10 95.8(5), C4–Te1–C10 92.6(5).

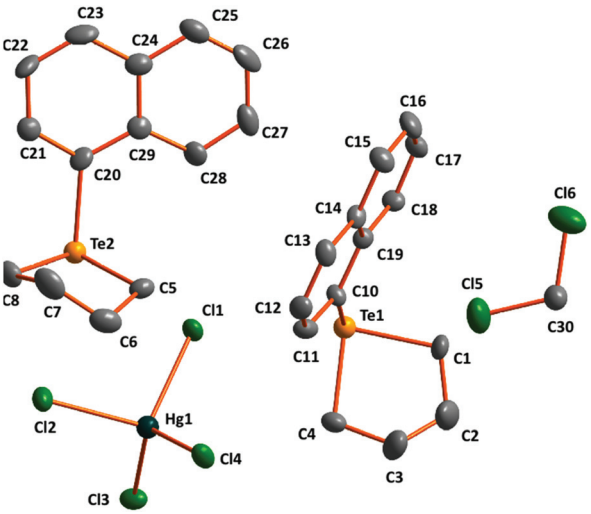

Fig. 4 The molecular structure of $[(C_{10}H_7)Te(CH_2)_4]_2[HgCl_4]\cdot CH_2Cl_2$ (**4**·CH_2Cl_2) indicating the numbering of atoms. Thermal ellipsoids have been drawn at 50% probability level. Hydrogen atoms have been omitted for clarity. Selected bond lengths (Å) and angles (°): Te1–C1 2.143(8), Te1–C4 2.140(8), Te1–C10 2.148(7), Te2–C5 2.153(8), Te2–C8 2.147(8), Te2–C20 2.132(8), C1–Te1–C4 84.0(3), C1–Te1–C10 94.5(3), C4–Te1–C10 97.9(3), C5–Te1–C8 85.1(3), C5–Te2–C20 98.5(3), C8–Te2–C20 94.6(3).

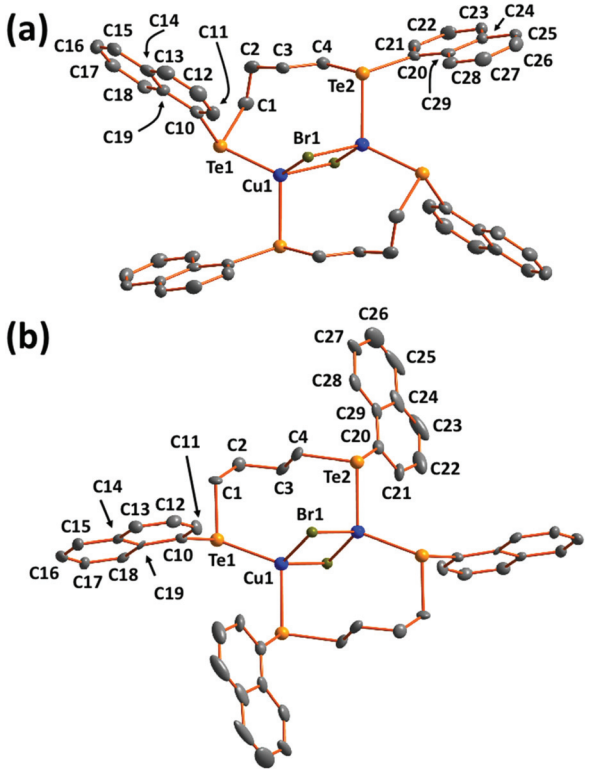

Fig. 5 The molecular structure of (a) the triclinic two polymorph and (b) the monoclinic polymorph of $[Cu_2(\mu\text{-}Br)_2\{\mu\text{-}(C_{10}H_7)Te(CH_2)_4Te(C_{10}H_7)\}_2]$ (**3a** and **3b**) indicating the numbering of atoms. Thermal ellipsoids have been drawn at 50% probability level. Hydrogen atoms have been omitted for clarity. Selected bond lengths (Å) and angles (°): **3a**: Cu1–Br1 2.486(2), $Cu1^a$–Br1 2.5215(13), Cu1–Te1 2.5552(12), $Cu1^a$–Te2 2.5958(14), Te1–C1 2.177(7), Te1–C10 2.130(7), Te2–C4 2.159(7), Te2–C20 2.129(6), Br1–Cu1–$Br1^a$ 103.29(4), Br1–Cu1–Te1 123.69(4), $Br1^a$–Cu1–Te1 106.26(5), $Br1^a$–$Cu1^a$–Te2 107.76(3), Br1–$Cu1^a$–Te2 99.08(4), Te1–Cu1–$Te2^a$ 113.36(4), Cu1–Te1–C1 100.75(19), Cu1–Te1–C10 105.66(19), $Cu1^a$–Te2–C20 106.89(16), C1–Te1–C10 98.0(3), C4–Te2–C20 98.6(2), C4–Te2–$Cu1^a$ 98.06(18), Cu1–Br1–$Cu1^a$ 76.71(4), C10–Te1–C1–C2 −18.7(5), Te1–C1–C2–C3 −68.1(6), C1–C2–C3–C4 −83.2(7), C2–C3–C4–Te2 +171.6(5), C3–C4–Te2–C20 +170.3(4); **3b**: Cu1–Br1 2.4433(18), $Cu1^a$–Br1 2.5495(18), Cu1–Te1 2.5493(15), $Cu1^a$–Te2 2.5652(16), Te1–C1 2.188(10), Te1–C10 2.132(10), Te2–C4 2.144(11), Te2–C20 2.105(12), Br1–Cu1–$Br1^a$ 108.48(6), Br1–Cu1–Te1 118.43(6), $Br1^a$–Cu1–Te1 107.15(6), Br1–$Cu1^a$–Te2 92.60(6), $Br1^a$–$Cu1^a$–Te2 115.02(6), Te1–Cu1–$Te2^a$ 111.62(6), Cu1–Te1–C1 112.3(3), Cu1–Te1–C10 105.1(3), $Cu1^a$–Te2–C20 107.8(3), C1–Te1–C10 90.0(4), C4–Te2–C20 99.4(3), C4–Te2–$Cu1^a$ 99.1(3), Cu1–Br1–$Cu1^a$ +71.52(6), C10–Te1–C1–C2 +178.5(8), Te1–C1–C2–C3 −67.8(11), C1–C2–C3–C4 −54.7(13), C2–C3–C4–Te2 +175.8(7), C3–C4–Te2–C20 +44.7(9).

The molecular structure and the crystal packing of **2** and **5** have similar features to those observed for other simple telluronium halogenide salts, as exemplified by Ph_3TeCl,[31] Ph_3TeBr,[32] and Ph_3TeI.[33] The three Te–C bonds in the cations of **2** and **5** are 2.122(10)–2.161(10) and 2.109(12)–2.168(13) Å, respectively and compare well with those in Ph_3TeX (X = Cl, Br, I).[31–33] The two Te···Br contacts in **2** or Te···Cl contacts in **5** [3.3419(5)–3.3651(5) and 3.219(3)–3.222(6) Å, respectively] expand the coordination polyhedron of the tellurium atom into a square pyramid (see Fig. 1S in the ESI†). Whereas in the solid state short Te···Cl contacts in Ph_3TeCl link the ion-pairs into dimers,[31a,c] in $Ph_3TeCl\cdot 1/2CHCl_3$,[31b] Ph_3TeBr,[32] and Ph_3TeI[33] the lattice is built up by ladder-like tetrameric units. By contrast, similar cation–anion contacts in **2** and **5** result in the formation of infinite chains. Further H···Np π interactions create three-dimensional supramolecular networks (see Fig. 1S in the ESI†).

The cation in **4**·CH_2Cl_2 expectedly shows a similar structure to **2** and **5** (see Fig. 4). The cations and anions are linked into a three-dimensional network through Te···Cl contacts of 3.290(2)–3.336(3) Å. The shortest H···Cl hydrogen bonds between the cation and the anion are 2.783(2)–2.983(3) Å. Furthermore, the solvent CH_2Cl_2 molecules also show hydrogen bonds of 2.915(2)–3.3036(3) Å to the telluronium cation. These solvent molecules also form dimers by two H···Cl contacts of 3.002(3) Å. The packing in the lattice is shown in Fig. 2S in the ESI.†

$[Cu_2(\mu\text{-}Br)_2\{\mu\text{-}(C_{10}H_7)Te(CH_2)_4Te(C_{10}H_7)\}_2]$ (3). $[Cu_2(\mu\text{-}Br)_2\{\mu\text{-}(C_{10}H_7)Te(CH_2)_4Te(C_{10}H_7)\}_2]$ (**3**) crystallizes as two polymorphs in space groups $P\bar{1}$ (**3a**) and $P2_1/c$ (**3b**). Their molecular structures together with the numbering of the atoms are presented in Fig. 5(a) and (b).

The Cu–Br bonds are somewhat shorter for **3a** [2.486(2)–2.5215(13) Å] and **3b** [2.4433(18)–2.5495(18) Å] than for $[Cu_2Br_2(dppb)_2]$ [dppb = bis(diphenylphosphino)butane] [2.5323(9) and 2.5726(7) Å].[26c] The Te–Cu–Te bond angles of **3a** and **3b** [113.36(4) and 111.62(6)°, respectively] are significantly smaller than the P–Cu–P angles of 125.03(5)° in $[Cu_2Br_2(dppb)_2]$.[26c]

It can be seen in Fig. 5 that the two polymorphs differ due to the conformations of the bridging ditelluroether ligands.

The motifs in the torsional angles C10–Te1–C1–C2, Te1–C1–C2–C3, C1–C2–C3–C4, C2–C3–C4–Te2, and C3–C4–Te2–C20 are − − − + + and + − − + + for **3a**, and **3b**, respectively (+ indicates the clockwise rotation about the central bond defining the torsional angle and − the anticlockwise rotation; for actual metrical values, see Fig. 5). This leads to differences in packing, as shown in Fig. 3S in the ESI.† The shortest Br···H hydrogen bond in **3a** is 3.0754(14) Å and those in **3b** are 2.9072(14) and 3.0439(12) Å.

Formation of $(C_{10}H_7)Te(CH_2)_4Te(C_{10}H_7)$ (1) and $[C_{10}H_7Te(CH_2)_4]_nX$ {*n* = 1, X = Br (2), Cl (5); *n* = 2, X = $[HgCl_4]$ (4)}

Although the syntheses of $RTe(CH_2)_nTeR$ (R = Me or Ph; n = 1, 3) by the reaction of RTe^- with organic dihalides $X(CH_2)_nX$ (X = Cl, Br) at low temperatures have been reported,[4b,c] the reaction involving $X(CH_2)_4X$ at room temperature seems to result in the preferential formation of the ionic telluronium halogenide $[RTe(CH_2)_4]X$ (R = *p*-$EtOC_6H_4$ or Ph).[4a] We have also observed that $(C_{10}H_7)Te(CH_2)_4Te(C_{10}H_7)$ (**1**) can be prepared with a moderate yield at −25 °C, but as the temperature of the reaction mixture rises to room temperature, an equally good yield of $[(C_{10}H_7)Te(CH_2)_4]Br$ (**2**) together with some **1** can be obtained.

Since it was possible that the prolonged reaction time even at low temperatures could result in the formation of $[(C_{10}H_7)Te(CH_2)_4]Br$ (**2**) in addition to that of $(C_{10}H_7)Te(CH_2)_4Te(C_{10}H_7)$ (**1**), we carried out two small-scale experiments in THF at −40 °C and monitored the products by ^{125}Te NMR spectroscopy. In one experiment, the reaction was discontinued after one hour. The reaction solution in THF was slightly cloudy, and the ^{125}Te NMR spectrum showed the main resonance at 352 ppm, which is due to **1**, with only a trace of the resonance at 666 ppm, which is due to the $[(C_{10}H_7)Te(CH_2)_4]^+$ cation of **2**. The latter resonance is known to be slightly soluble in THF. Another reaction was discontinued after six hours. In this solution, there was a clear presence of the precipitate of **2**. The ^{125}Te NMR spectrum showed that the concentration of **2** had also increased somewhat during the prolonged stirring time at −40 °C, though **1** was still the main product. It can be concluded that both **1** and **2** are formed also at low temperatures, but under these conditions the formation of **1** is faster than that of **2**.

Since it is conceivable that the formation of **1** and **2** can take place concurrently, as shown in Scheme 1, or sequentially, as shown in Scheme 2, we decided to carry out revPBE/def2-TZVPP calculations both at 298 K and at 200 K. The energy profiles of the three different reactions in question at room temperature (298 K) are shown in Fig. 6.

The first step in both reactions is the formation of acyclic $(C_{10}H_7)Te(CH_2)_4Br$ from $Li^+[Te(C_{10}H_7)^-]$ and $Br(CH_2)_4Br$. This reaction is relatively straight-forward and since it is common for the formation of both **1** and **2**, we used it as a starting point for our calculations. It can be seen from the Gibbs energy values shown in Fig. 6 that in the formation of both **1** and **2**, the driving force is the formation of solid salts, namely LiBr(s) in the case of **1**, and that of **2** itself. The activation energies are reasonably low and relatively close to each other with that for the reaction leading to **1** (shown in green) slightly higher than that for the reaction leading to **2** (shown in red). The total energy of the formation of **2** is somewhat more favourable than that of **1**. Furthermore, the conversion of **1** to

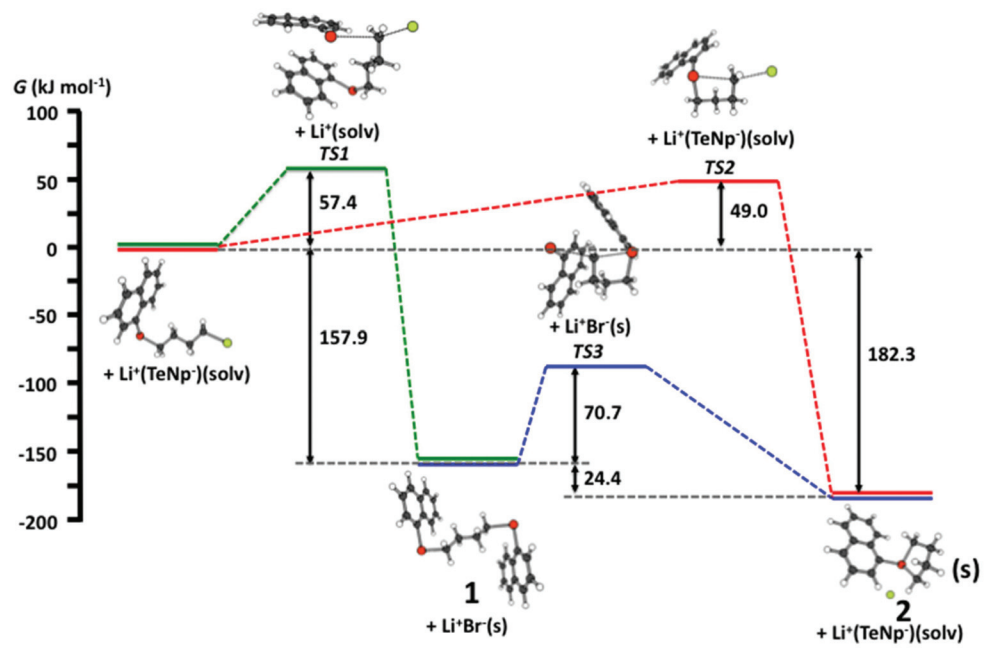

Fig. 6 revPBE/def2-TZVPP reaction profiles of the formation of $(C_{10}H_7)Te(CH_2)_4Te(C_{10}H_7)$ (**1**) (shown in green) and of $[(C_{10}H_7)Te(CH_2)_4^+]Br$ (**2**) (shown in red) from $C_{10}H_7Te(CH_2)_4Br$. The reaction profile of the decomposition of **1** to **2** (shown in blue). Each of the three transition states *TS1*–*TS3* show only one imaginary frequency.

2 goes *via* a higher activation barrier (shown in blue). All these findings support the earlier conclusion that at room temperature the quaternation at tellurium and the formation of the telluronium salt are faster than the reaction of $RTe(CH_2)_4Br$ with another equivalent of RTe^-.[4a]

We have also computed the activation barriers for reactions *via* the transition states *TS1* and *TS2* at 200 K. The activation energy for the formation of ditelluroether **1** (transition state *TS1*) was lowered to 32.1 kJ mol^{-1}, while the activation barriers for the formation of the telluronium bromide **2** (transition state *TS2*) and that for the decomposition of the ditelluroether **1** to the telluronium bromide **2** (transition state *TS3*) remained approximately unchanged. This is consistent with our experimental observation that at low temperatures the reaction of $(C_{10}H_7)Te^-$ with $Br(CH_2)_4Br$ affords $(C_{10}H_7)Te(CH_2)_4Te(C_{10}H_7)$ (**1**) faster than $[(C_{10}H_7)Te(CH_2)_4]Br$ (**2**). While in principle spontaneous, the decomposition of **1** to **2** does not seem to be a significant alternative route.

However, we tested the possibility of the conversion of **1** to **2** by adding an excess of LiBr to the THF solution of **1** and stirring the mixture for several days. Only trace amounts of **2** were formed. It further supports the conclusion that **2** is mainly formed concurrently with **1** and that the relative rates of the formation of the two products are dependent on the temperature.

In contrast, the treatment of **1** with $HgCl_2$ resulted in the formation of $[(C_{10}H_7)Te(CH_2)_4]_2[HgCl_4]$ (**4**) in a good yield. The likely reaction is presented in eqn (1).

$$2(C_7H_{10})Te(CH_2)_4Te(C_{10}H_7) + 2HgCl_2 \rightarrow [(C_{10}H_7)Te(CH_2)_4]_2[HgCl_4] + [Hg\{Te(C_{10}H_7)\}_2] \quad (1)$$

It is possible that the reaction is fast due to the catalytic effect of mercury resulting in the formation of the salt **4**. We also tested a related reaction by treating **1** with $CuCl_2$. The ^{125}Te NMR spectrum of the reaction mixture in CH_2Cl_2 indicates that this reaction affords the chloride salt **5** and approximately a half equivalent of $(C_{10}H_7)TeTe(C_{10}H_7)$. Both products could be isolated and structurally characterized. A possible path of the reaction involves the reduction of Cu^{2+} with the consequent oxidation of $(C_{10}H_7)Te^-$ to $(C_{10}H_7)TeTe(C_{10}H_7)$ (see eqn (2)):

$$(C_{10}H_7)Te(CH_2)_4Te(C_{10}H_7) + CuCl_2 \rightarrow [(C_{10}H_7)Te(CH_2)_4]Cl + \frac{1}{2}(C_{10}H_7)TeTe(C_{10}H_7) + CuCl \quad (2)$$

Conclusions

The low-temperature preparation of a rare new ditelluroether $(C_{10}H_7)Te(CH_2)_4Te(C_{10}H_7)$ (**1**) from naphthyl bromide, *n*-butyl lithium, elemental tellurium, and 1,4-dibromobutane has been described. The crystal structure of **1** shows two independent molecules, which are linked by Te···Te secondary bonding interactions and Te···H hydrogen bonds.

Upon prolonged stirring of the reaction solution during which time the temperature rose to the room temperature, a telluronium salt $[(C_{10}H_7)Te(CH_2)_4]Br$ (**2**) has been observed and isolated. A similar cation is obtained in the reactions of **1** with M(II) metal salts $HgCl_2$ and $CuCl_2$, which form $[(C_{10}H_7)Te(CH_2)_4]_2[HgCl_4]$ (**4**) and $[(C_{10}H_7)Te(CH_2)_4]Cl$ (**5**), respectively. The two $[C_{10}H_7Te(CH_2)_4]X$ [X = Br (**2**), Cl (**5**)] salts are isomorphous. The cation–anion contacts in **2** and **5** result in the formation of infinite chains.

The dinuclear complex $[Cu_2(\mu\text{-}Br)_2\{\mu\text{-}(C_{10}H_7)Te(CH_2)_4Te(C_{10}H_7)\}_2]$ (**3**) was formed by the reaction of **1** with CuBr. It crystallizes as two polymorphs **3a** and **3b**, which both show a similar bridging arrangement of both the ditelluroether ligands and bromides between two Cu(I) centers. There are, however, marked differences in the conformations of the ditelluroether ligands and in the packing of the complexes.

The revPBE/def2-TZVPP calculations of the reaction profiles indicate that **1** and **2** are formed concurrently. While both reactions are spontaneous, the total Gibbs energy change for the formation of **1** is somewhat less favourable than for that of **2**. The driving force for the reactions is the formation of solid LiBr in the case of **1** and the salt **2** itself in the latter case. While at room temperature the activation energy in the formation of **1** is higher than that of **2**, at low temperatures the situation is reversed. It can therefore be concluded that at low temperatures the formation of **1** from $(C_{10}H_7)Te^-$ and $Br(CH_2)_4Br$ is faster than that of **2**, but at the room temperature the telluronium salt **2** is somewhat favoured over the ditelluroether **1**. While the calculations indicate that the decomposition of **1** to **2** upon interaction with Br^- is energetically possible, the activation energy of the reaction is somewhat higher than in the concurrent reactions, which renders the decomposition of **1** less likely. Furthermore, a separate experiment has shown that there is indeed little or no evidence for the formation of **2** from **1**.

Acknowledgements

Financial support from the Academy of Finland (The Inorganic Materials Chemistry Graduate Program) (M. J. P.) is gratefully acknowledged. We are also grateful to Finnish CSC-IT Center for Science Ltd for their generous provision of computational resources.

Notes and references

1 N. Petragnani and G. Schill, *Chem. Ber.*, 1970, **103**, 2271–2273.
2 (*a*) A. K. Singh and V. Srivastava, *J. Coord. Chem.*, 1992, **27**, 237–253; (*b*) E. G. Hope and W. Levason, *Coord. Chem. Rev.*, 1993, **122**, 109–170; (*c*) A. K. Singh and S. Sharma, *Coord. Chem. Rev.*, 2000, **209**, 49–98; (*d*) W. Levason, S. D. Orchard

and G. Reid, *Coord. Chem. Rev.*, 2002, **225**, 159–199; (*e*) A. J. Barton, A. R. J. Genge, N. J. Hill, W. Levason, S. D. Orchard, B. Patel, G. Reid and A. J. Ward, *Heteroat. Chem.*, 2002, **13**, 550–560; (*f*) W. Levason and G. Reid, in *Handbook of Chalcogen Chemistry: New Perspectives in Sulfur, Selenium and Tellurium*, ed. F. A. Devillanova, RSC Publishing, U. K., 2007, ch. 2.2, pp. 81–106; (*g*) A. Panda, *Coord. Chem. Rev.*, 2009, **253**, 1947–1965.

3 (*a*) D. Seebach and A. K. Beck, *Chem. Ber.*, 1975, **108**, 314–321; (*b*) C. H. W. Jones and R. D. Sharma, *Organometallics*, 1986, **5**, 805–808; (*c*) L. Torres C, *J. Organomet. Chem.*, 1990, **381**, 69–78.

4 (*a*) K. G. K. De Silva, Z. Monsef-Mirzai and W. R. McWhinnie, *J. Chem. Soc., Dalton Trans.*, 1983, 2143–2146; (*b*) E. G. Hope, T. Kemmitt and W. Levason, *Organometallics*, 1987, **6**, 206–207; (*c*) E. G. Hope, T. Kemmitt and W. Levason, *Organometallics*, 1988, **7**, 78–83.

5 H. M. K. K. Pathirana and W. R. McWhinnie, *J. Chem. Soc., Dalton Trans.*, 1986, 2003–2005.

6 (*a*) M. de Matheus, L. Torres, J. F. Piniella and C. Miravitlles, *Acta Crystallogr., Sect. C: Cryst. Struct. Commun.*, 1991, **47**, 1264–1266; (*b*) A. K. Singh, M. Kadarkaraisamy, J. E. Drake and R. J. Butcher, *Inorg. Chim. Acta*, 2000, **304**, 45–51; (*c*) S. Gulati, S. Pundir, S. Kumar and K. K. Bhasin, *Phosphorus, Sulfur Silicon Relat. Elem.*, 2015, **190**, 1509–1517.

7 (*a*) T. Kemmitt, W. Levason and M. Webster, *Inorg. Chem.*, 1989, **28**, 692–696; (*b*) W.-F. Liaw, Y.-C. Horng, D.-S. On, C.-Y. Chuang, C.-K. Lee, G.-H. Lee and S.-M. Peng, *J. Chin. Chem. Soc.*, 1995, **42**, 59–65; (*c*) B. L. Khandelwal, A. Khalid, A. K. Singh, T. P. Singh and S. Karthikeyan, *J. Organomet. Chem.*, 1996, **507**, 65–68; (*d*) J. E. Drake, J. Yang, A. Khalid, V. Srivastava and A. K. Singh, *Inorg. Chim. Acta*, 1997, **254**, 57–62; (*e*) W. Levason, S. D. Orchard, G. Reid and V.-A. Tolhurst, *J. Chem. Soc., Dalton Trans.*, 1999, 2071–2076; (*f*) A. J. Barton, W. Levason, G. Reid and V.-A. Tolhurst, *Polyhedron*, 2000, **19**, 235–240; (*g*) S. Jing, C. P. Morley, C. A. Webster and M. Di Vaira, *Dalton Trans.*, 2006, 4335–4342; (*h*) S. Jing, C. P. Morley, C. A. Webster and M. Di Vaira, *J. Organomet. Chem.*, 2008, **693**, 2310–2316.

8 (*a*) W.-F. Liaw, C.-H. Lai, S.-J. Chiou, Y.-C. Horng, C.-C. Chou, M.-C. Liaw, G.-H. Lee and S.-M. Peng, *Inorg. Chem.*, 1995, **34**, 3755–3759; (*b*) K. George, C. H. de Groot, C. Gurnani, A. L. Hector, R. Huang, M. Jura, W. Levason and G. Reid, *Chem. Mater.*, 2013, **25**, 1829–1836; (*c*) K. Kobayashi, H. Masu, A. Shuto and K. Yamaguchi, *Chem. Mater.*, 2015, **17**, 6666–6673.

9 M. J. Poropudas, L. Vigo, R. Oilunkaniemi and R. S. Laitinen, *Dalton Trans.*, 2013, **42**, 16868–16877, and references there in.

10 (*a*) J. L. Hartwell, *Org. Synth.*, 1944, **24**, 22–25; (*b*) J. L. Hartwell, *Org. Synth.*, 1955, **3**, 185–188.

11 M. J. Collins and G. J. Schrobilgen, *Inorg. Chem.*, 1985, **24**, 2608–2614.

12 G. M. Sheldrick, *Acta Crystallogr., Sect. A: Fundam. Crystallogr.*, 2008, **64**, 112–122.

13 T. Pullmann, B. Engendahl, Z. Zhang, M. Hölscher, A. Zanotti-Gerosa, A. Dyke, G. Franciò and W. Leitner, *Chem. – Eur. J.*, 2010, **16**, 7517–7526.

14 *The ORCA program, version 3.0.3*; F. Neese, *WIREs Comput. Mol. Sci.*, 2012, **2**, 73.

15 (*a*) J. P. Perdew, K. Burke and M. Ernzerhof, *Phys. Rev. Lett.*, 1996, **77**, 3865–3868; (*b*) J. P. Perdew, K. Burke and M. Ernzerhof, *Phys. Rev. Lett.*, 1997, **78**, 1396; (*c*) Y. Zhang and W. Yang, *Phys. Rev. Lett.*, 1998, **80**, 890; (*d*) J. P. Perdew, K. Burke and M. Enrzernhof, *Phys. Rev. Lett.*, 1998, **80**, 891.

16 (*a*) A. Schäfer, H. Horn and R. Ahlrichs, *J. Chem. Phys.*, 1992, **97**, 2571–2577; (*b*) F. Weigend and R. Ahlrichs, *Phys. Chem. Chem. Phys.*, 2005, **7**, 3297–3305; (*c*) D. Andrae, U. Häußermann, M. Dolg, H. Stoll and H. Preuß, *Theor. Chim. Acta*, 1990, **77**, 123–141; (*d*) F. Weigend, *Phys. Chem. Chem. Phys.*, 2006, **8**, 1057–1065.

17 F. Neese, *J. Comput. Chem.*, 2003, **24**, 1740–1747.

18 (*a*) S. Grimme, S. Ehrlich and L. Goerigk, *J. Comput. Chem.*, 2011, **32**, 1456–1465; (*b*) S. Grimme, J. Antony, S. Ehrlich and H. Krieg, *J. Chem. Phys.*, 2010, **132**, 154104–154118.

19 (*a*) A. Klamt and G. Schüürmann, *J. Chem. Soc., Perkin Trans. 2*, 1993, 799–805; (*b*) S. Sinnecker, A. Rajendran, A. Klamt, M. Diedenhofen and F. Neese, *J. Phys. Chem. A*, 2006, **110**, 2235–2245.

20 (*a*) R. Dovesi, R. Orlando, A. Erba, C. M. Zicovich-Wilson, B. Civalleri, S. Casassa, L. Maschio, M. Ferrabone, M. De La Pierre, P. D'Arco, Y. Noël, M. Causà, M. Rérat and B. Kirtman, *Int. J. Quantum Chem.*, 2014, **114**, 1287–1317; (*b*) R. Dovesi, V. R. Saunders, C. Roetti, R. Orlando, C. M. Zicovich-Wilson, F. Pascale, B. Civalleri, K. Doll, N. M. Harrison, I. J. Bush, P. D'Arco, M. Llunell, M. Causà and N. Noël, *CRYSTAL14, CRYSTAL14 User's Manual*, University of Torino, Torino, 2014.

21 (*a*) J. P. Perdew, M. Ernzerhof and K. Burke, *J. Chem. Phys.*, 1996, **105**, 9982–9985; (*b*) C. Adamo and V. Barone, *J. Chem. Phys.*, 1999, **110**, 6158–6170.

22 M. F. Peintinger, D. Vilela Oliveira and T. Bredow, *J. Comput. Chem.*, 2013, **34**, 451–459.

23 S. M. Närhi, J. Kutuniva, M. K. Lajunen, M. K. Lahtinen, H. M. Tuononen, A. J. Karttunen, R. Oilunkaniemi and R. S. Laitinen, *Spectrochim. Acta, Part A*, 2014, **117**, 728–738.

24 (*a*) S. Grimme, *J. Comput. Chem.*, 2006, **27**, 1787–1799; (*b*) L. A. Burns, A. Vazquez-Mayagoitia, B. G. Sumpter and C. D. Sherrill, *J. Chem. Phys.*, 2011, **134**, 084107.

25 (*a*) F. Pascale, C. M. Zicovich-Wilson, F. López Gejo, B. Civalleri, R. Orlando and R. Dovesi, *J. Comput. Chem.*, 2004, **25**, 888–897; (*b*) C. M. Zicovich-Wilson, F. Pascale, C. Roetti, V. R. Saunders, R. Orlando and R. Dovesi, *J. Comput. Chem.*, 2004, **25**, 1873–1881.

26 (*a*) J. M. Townsend, J. F. Blount, R. C. Sun, S. Zawoiski and D. Valentine Jr., *J. Org. Chem.*, 1980, **45**, 2995–2999; (*b*) S. Jing, T. Yin, Y.-X. Wang, Y.-L. Song, H.-G. Zheng and

X.-Q. Xin, *Chin. J. Inorg. Chem.*, 2002, **18**, 1169–1172; (*c*) Effendy, C. Di Nicola, M. Fianchini, C. Pettinari, B. W. Skelton, N. Somers and A. H. White, *Inorg. Chim. Acta*, 2005, **358**, 763–795; (*d*) Y.-H. Deng, Y.-L. Yang and X.-J. Yang, *Z. Kristallogr. – New Cryst. Struct.*, 2006, **221**, 316–318; (*e*) J.-X. Li, Z.-X. Du, H.-Q. An, J. Zhou, J.-X. Dong, S.-R. Wang, B.-L. Zhu, S.-M. Zhang, S.-H. Wu and W.-P. Huang, *J. Mol. Struct.*, 2009, **935**, 161–166; (*f*) X. Zhang, L. Song, M. Hong, H. Shi, K. Xu, Q. Lin, Y. Zhao, Y. Tian, J. Sun, K. Shu and W. Chai, *Polyhedron*, 2014, **81**, 687–694.

27 E. Schulz Lang, R. A. Burrow and E. T. Silveira, *Acta Crystallogr., Sect. C: Cryst. Struct. Commun.*, 2002, **58**, o397–0398.

28 B. L. Khanderwal, S. K. Jain and F. J. Berry, *Inorg. Chim. Acta*, 1982, **59**, 193–196.

29 (*a*) M. N. Ponnuswamy and J. Trotter, *Acta Crystallogr., Sect. C: Cryst. Struct. Commun.*, 1984, **40**, 1671–1673; (*b*) A. Beleaga, V. R. Bojan, A. Pöllnitz, C. I. Rat and C. Silvestru, *Dalton Trans.*, 2011, **40**, 8830–8838.

30 J. Emsley, *The Elements*, Oxford University Press, New York, 3rd edn, 1998.

31 (*a*) R. F. Ziolo and M. Extine, *Inorg. Chem.*, 1980, **19**, 2964–2967; (*b*) M. J. Collins, J. A. Ripmeester and J. F. Sawyer, *J. Am. Chem. Soc.*, 1988, **110**, 8583–8590; (*c*) F. Hu, C. Xu, H.-T. Shi, Q. Chen and Q.-F. Zhang, *Acta Crystallogr., Sect. E: Struct. Rep. Online*, 2013, **69**, o1171.

32 S. M. Närhi, R. Oilunkaniemi and R. S. Laitinen, *Acta Crystallogr., Sect. E: Struct. Rep. Online*, 2013, **69**, o1666.

33 W.-W. du Mont, J. Jeske and P. G. Jones, *Phosphorus, Sulfur Silicon Relat. Elem.*, 2010, **185**, 1243–1249.